Proposal

Electron pair spectrometer at the J-PARC 50-GeV PS to explore the chiral symmetry in QCD

April 28, 2006
June 07, 2006 rev.1

S. Yokkaichi[1], H. En'yo, M. Naruki, R. Muto, T. Tabaru

RIKEN

K. Ozawa, H. Hamagaki

Center for Nuclear Study, Graduate School of Science, University of Tokyo

K. Shigaki

Graduate School of Science, Hiroshima University

S. Sawada, M. Sekimoto

High Energy Accelerator Research Organization (KEK)

F. Sakuma, K. Aoki

Department of Physics, Kyoto University

[1]spokesperson, yokkaich@riken.go.jp

Contents

1 Introduction

The spontaneous breaking of the chiral symmetry is playing an essential role in QCD. Effective quark mass which constitutes hadrons is due to the braking. In hot (finite temperature) and/or dense (finite density) matter, the chiral phase transition takes place and the broken symmetry is restored. It is predicted by Lattice QCD that the deconfinement of quark and the chiral phase transition would occur at the same temperature. Quark condensate $\langle\bar{q}q\rangle$ is an order parameter of the chiral phase transition. As temperature (density) increases, the absolute value of $\langle\bar{q}q\rangle$ decreases and finally goes to zero at the critical temperature (density). Unfortunately $\langle\bar{q}q\rangle$ itself is not an observable, however, the spectral properties of hadrons like the mass and the decay width are expected to change sensitively to the $\langle\bar{q}q\rangle$ value. Namely the property of hadrons in the hot/dense matter is a good measure of the chiral symmetry restoration in the matter.

There have been many theoretical approaches to this problem[1] and some experiments already detected the modification of hadron in nuclear matter. At high temperature, the CERES experiment at CERN-SPS observed the change of low-mass e^+e^- spectra which suggests the modification of vector mesons in Pb-Au collision[2]. Also at CERN-SPS, the NA60 experiment measured low-mass $\mu^+\mu^-$ spectra and recently reported the modification of ρ meson in In-In collision[3]. The KEK-PS E325 experiment [4, 5, 6, 7], which was carried out by a collaboration including a part of the authors, measured the e^+e^- and K^+K^- decay of light vector mesons ($\rho/\omega/\phi$) made by the 12–GeV proton induced reaction in the target nucleus. They also detected the modification of the vector-meson invariant mass spectra in the e^+e^- channel with higher mass resolution than the CERES and NA60 experiments. The results of E325 are explained in the following section.

In the lower energy region as several GeV, TAGX at INS (KEK-TANASHI) detected the ρ meson modification in $\pi^+\pi^-$ channel in $\gamma + {}^3\mathrm{He}/{}^{12}\mathrm{C}$ reaction[8]. In $\pi^+\pi^-$ channel, the data measured by CHAOS at TRIUNF[9] suggested the modified σ meson in various nuclear targets made by the pion induced reaction. CB at AGS[10] also reported similar effect in $\pi^0\pi^0$ channel. The LEPS group at Spring-8 measured $\phi \to K^+K^-$ and the A-dependence of the ϕ-production cross section in γ + A reaction. They reported the medium effect against ϕ production and ϕ-N interaction. The spectral modification of ω meson was measured by the CBELSA/TAPS experiment in $\pi^0\gamma$ decay channel[12]. Dielectron measurement experiment in the energies are ongoing by HADES at GSI and CLAS-G7 at JLab.

It can be said that the existence of the hadron modification in medium has been established by these experimental results. However, the origin of the

modification is not clarified yet. There are also many explanation unrelated to the chiral symmetry. To investigate the problem, we propose to construct new spectrometer at "multi-purpose high momentum beam line" at J-PARC 50-GeV PS. The main aim of the spectrometer is a measurement of e^+e^- pair from the p+A reaction to investigate the chiral symmetry around the normal nuclear matter density as same as E325, with definitely higher statistics and possibly improved mass resolution.

In section 2 we discuss our physics motivation, related experiments and the main goal of the proposed experiment. At the first stage, we aim to collect around 10^5 of ϕ meson in e^+e^- channel for each nuclear target. The statistics are 100 times as large as the KEK–PS E325 experiment collected. When we collect such amount of ϕ meson , we can also collect ρ/ω meson about 10 times as much as ϕ meson in e^+e^- channel at the same time. Furthermore, approximately 1000 of J/ψ can also be collected when 50–GeV proton beam is used.

To collect such statistics in 100 shifts (33 days) of beam time, we have to use the high intensity primary proton beam of which intensity is 10^{10} proton per spill and energy is 30 or 50 GeV with thin target around 0.1% interaction length. To cope with 10^7 Hz (10 MHz) of interaction rate at the target, we have to construct a new spectrometer using new technologies. The design of our proposed spectrometer and experimental details are described in section 3. The design work is performed on the basis of the experimental experiences of the E325 experiment.

At the next stage of the proposed experiment, measurement of J/ψ , K^*, D, σ and so on using this spectrometer with some upgrading should be considered. When heavy-ion beam is available in J-PARC, we can explore the chiral symmetry in higher density, which may be the highest density in humankind have ever made on earth. By such measurements of various hadrons in same density environment, we will have deeper insight into modification of hadrons and further, the chiral symmetry and QCD itself.

2 Physics

As described in previous section, both the finite temperature and the finite density environment are important to investigate the chiral symmetry in QCD. In J-PARC, we put emphasis on the latter environment. The proton (or secondary beam hadron) induced reactions make mesons in target nucleus, which bring the information of the environment around normal nuclear density. Heavy ion collisions around 20∼25 GeV/nucleon are expected to achieve the high baryon density 5∼10 times as large as the normal nuclear density. Of course such energy region was investigated by the AGS (∼ 12 GeV/nucleon) and recently SPS (20 ∼ 30 GeV/nucleon) heavy ion experiments, however, these experiments did not use the electron probe, which less interact in final state. Only CBM experiment (GSI future project) [19] is competing with us in this energy region.

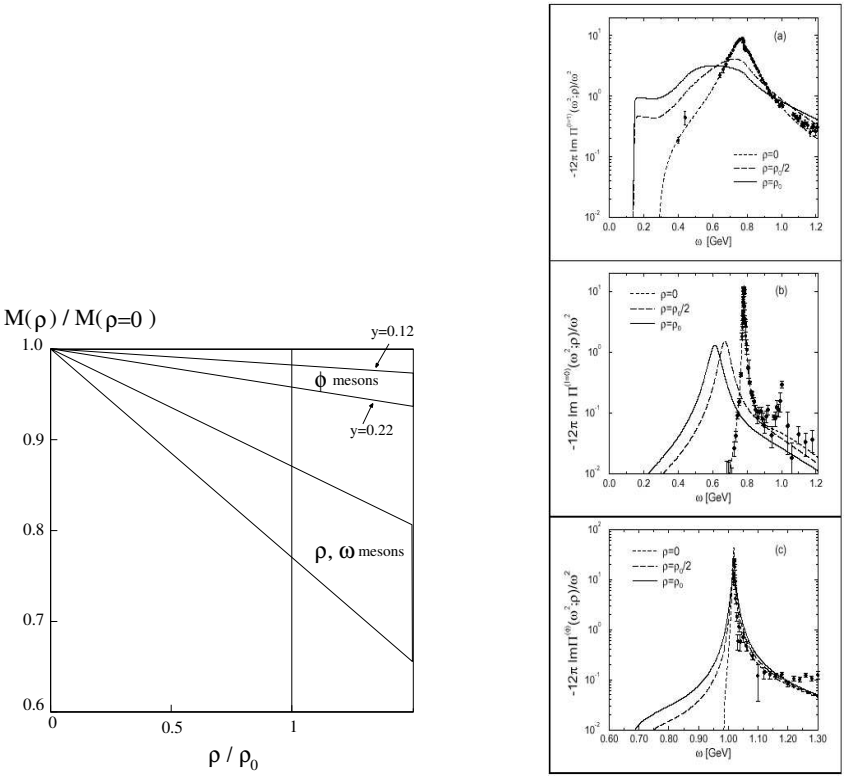

Figure 1: mass modification of vector mesons in finite density predicted by Hatsuda and Lee [13](left) and Klingl *et al.* [15] (right: upper is for ρ, middle is for ω and lower is for ϕ meson).

The chiral symmetry restoration in finite density has been studied in many theoretical methods. Hatsuda and Lee studied using the QCD sum rule and calculate the mass of $\rho/\omega/\phi$ mesons and predicted 10$\sim$20% decreasing for ρ/ω and 2$\sim$4 % for ϕ at normal nuclear density[13] as shown in Fig1. Hayashigaki studied the mass of J/ψ and D meson also using QCD sum rule and predicted about 0.1$\sim$0.2% decreasing for J/ψ and 2$\sim$3% for D meson also at the normal nuclear density[14]. Klingl *et al.* calculated the downward mass-shift and even mass broadening of $\rho/\omega/\phi$ in dense matter[15]. Furthermore, they also predicted the width-broadening of ϕ meson by a factor of ten[16] at normal nuclear density, by including the in-medium kaon spectral change. Some trials using lattice QCD have been made recently although such approaches using lattice for the finite density is more difficult than for the finite temperature. For example, Muroya, Nakamura and Nonaka calculated the mass of π and ρ mesons in finite chemical potential, and found the mass of ρ decreases as the chemical potential increases in the color-SU(2) QCD[17].

In the following subsections, we review the predecessor experiment KEK–PS E325 and our goal in the proposed experiment.

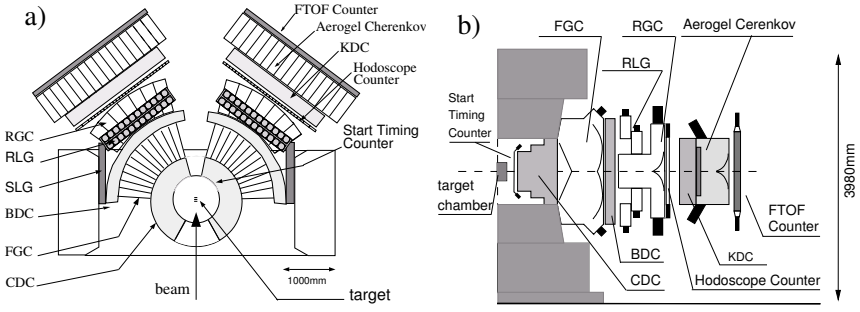

Figure 2: E325 spectrometer: top view and vertical cross section.

2.1 Predecessor experiment KEK–PS E325

The experiment KEK–PS E325 was proposed in 1993 and the construction was started in 1996 at the EP1–B primary beam line at KEK–PS. Data taking was started on the May, 1997 and completed on the March, 2002.

The spectrometer[18] was designed to detect the relatively slowly-moving vector mesons, because such mesons expected to spend longer time in nuclei after they are produced in proton-induced reaction and to have larger probability of decay inside nuclear matter. Possible spectral change depends on

the number of decayed meson in medium, thus slowly moving mesons and larger size nuclei are desired. The spectrometer mainly covered the backward region in the center-of-mass system. Schematic picture of the spectrometer is shown in Fig.2

In order to reduce the electron background from the γ conversion in the target material, typical radiation length of each target is set around 0.5% radiation length in order to balance the number of e^+e^- pair from π^0 Dalitz decays and that from the γ conversion in the target material.

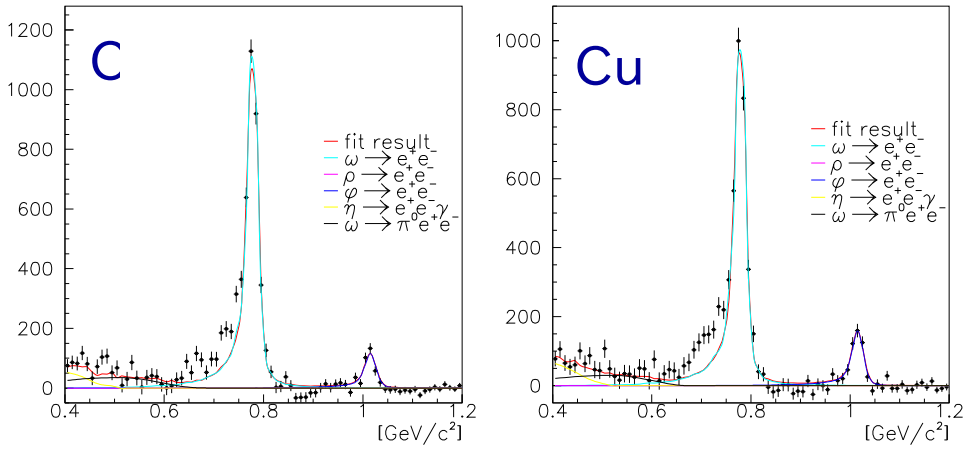

Figure 3: Invariant mass spectra in e^+e^- channel observed by E325. left is for carbon target and right is for copper target, after the background subtraction.

In order to compensate such thin targets and also small branching ratio into lepton channels (order of $10^{-4} \sim 10^{-5}$), high intensity primary beam was used to collect the high statistics. Typical beam intensity was 10^9 proton per spill and typical interaction rate on the targets was around 1 MHz, because the interaction length of such targets were around 0.1∼0.2%.

The experiment has been detected the modification of vector-meson spectra using e^+e^- decay. Here we explain the recent results, mainly from the data taken in 2001∼2002. As shown in Fig. 3 based on the analysis in the reference[5], significant excesses are found in the low-mass side of the usual $\omega(783)$ peak, which cannot be explained using known hadronic sources. Meson mass shape used in the fit are relativistic Breit-Wigner shape and distorted by the detector simulation taking account of the experimental effect like the energy loss and multiple scattering of electrons in the detectors,

external bremsstrahlung, detector acceptances, etc. Distortion due to the internal radiative correction for the leptonic decay is also taken into account. Combinatorial background is evaluated by the event mixing method.

The ω mesons have a longer life ($\sim$24 fm) relatively than ρ meson ($\sim$1.3 fm). Therefore more than 90% of ω are expected to decay in free space outside nucleus in which it is created and make such clear peak around 780 MeV/c^2 . On the other hand, ρ meson amplitude is very small as a result of the fit. It should be noted that the fit is performed with the hadronic shape in vacuum, in other word, unmodified. Therefore, the excess could be made by 'modified' ρ mesons decayed in nuclei.

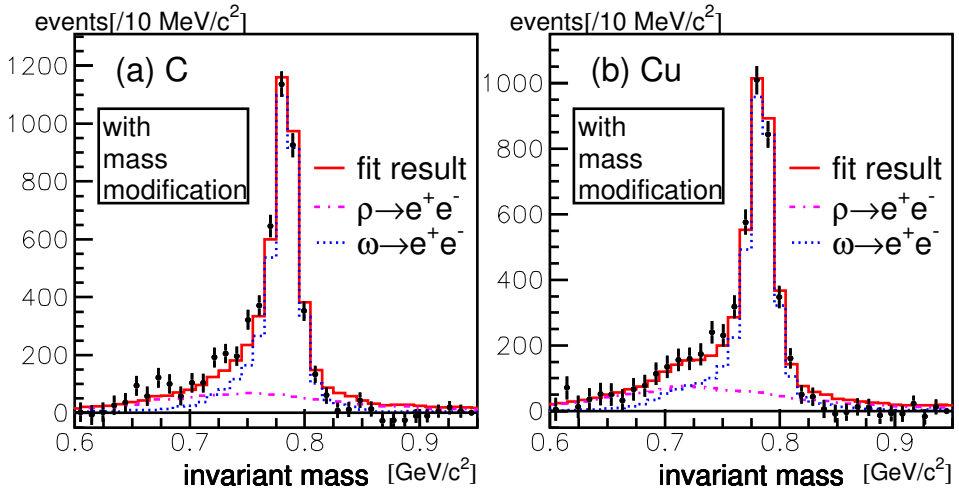

Figure 4: Model-fitting results of the invariant mass spectra in e^+e^- channel observed by E325. a) is for carbon and b) is for copper targets. Solid lines are best fit results.

To understand the shape observed including the nuclear size effect and velocity dependence, it is performed that the Monte Carlo type model calculation based on the prediction by Hatsuda and Lee[13]. Mesons are generated at the incident surface of the nucleus, having the measured momentum distribution, fly through the nucleus and decay following own life. If the decay point is inside nuclei, the mass is decreased by the predicted form: $m^*/m_0 = 1-k(\rho(r)/\rho_0)$. The nuclear matter density $\rho(r)$ follows the Woods-Saxon formula. The predicted value of the shift parameter k = 0.16 $\pm$ 0.06. And m^* is modified mass, m_0 is mass in vacuum and ρ_0 is a normal nuclear density. By this model calculation, the spectra are explained like as shown in Fig.4 with the modified shapes of ρ and ω. The shift parameter k is determined as 0.092 $\pm$ 0.002 by the fit, where k is assumed as common for C

and Cu target.

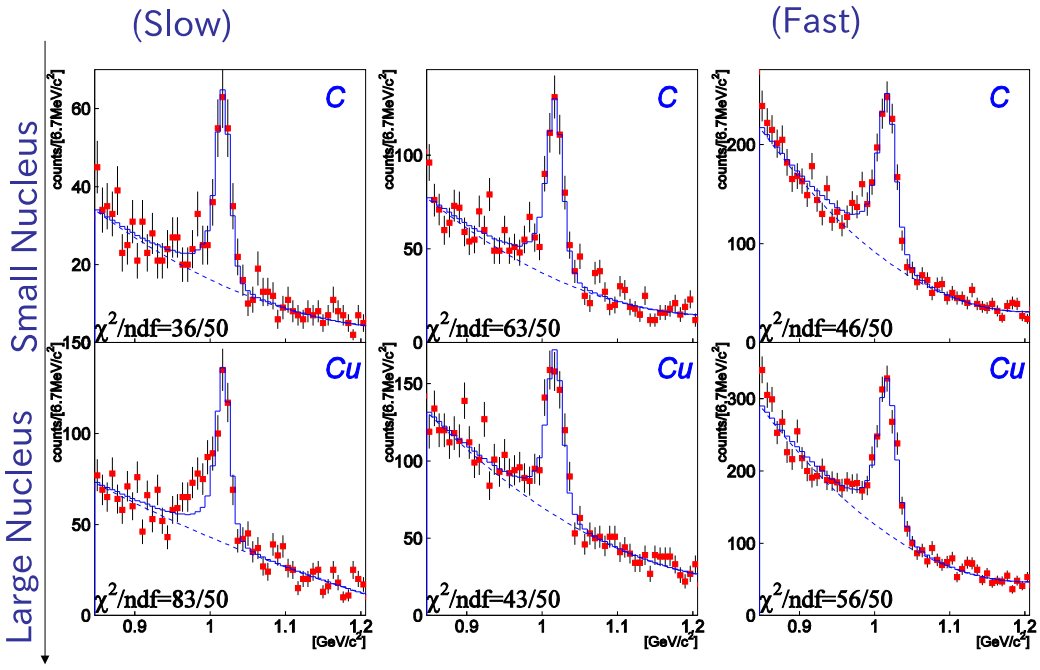

Figure 5: Invariant mass spectra of $\phi \to e^+e^-$ observed by E325. Upper panels are for carbon and lower are for copper targets. The data are divided by the meson velocity, slower ($\beta\gamma < 1.25$), middle ($1.25 < \beta\gamma < 1.75$) and faster ($1.75 < \beta\gamma$) component as shown in left, middle and right panels, respectively. Only the data shown in the lower-left panel have significant excess over the ϕ meson shape and the quadratic background curve.

For ϕ meson case, similar analysis was performed and the excess is observed only the slowly moving component in larger nuclear target as shown in Fig.5 from the reference [6]. The result is consistent with a view that almost all mesons, which are produced in nuclei with a few GeV of momentum, should decay outside the nucleus or nuclear matter and only limited number of mesons could decay inside nucleus with mass-modification by density effect, because the mean life is relatively longer than the nuclear size. The velocity-dependence analysis for ρ/ω meson case is also desired and ongoing.

The number of mesons in the excess is calculated by subtracting unmodified shape distorted by the detector simulation from the data and plotted in the left panel of Fig. 6. Supposing the excess consists of modified ϕ meson , the ratio $N_{excess}/(N_{excess} + N_\phi)$ means the fraction of $\phi \to e^+e^-$ decay inside nucleus among the total $\phi \to e^+e^-$ decays. The lines in the figure are the

results of the toy model calculation similar the ρ/ω meson case, including not only the mass decreasing but also the width broadening. Because the statistics are limited, it is difficult to distinguish the two value of the OZI breaking parameter y (see fig1) in the theoretical prediction[13].

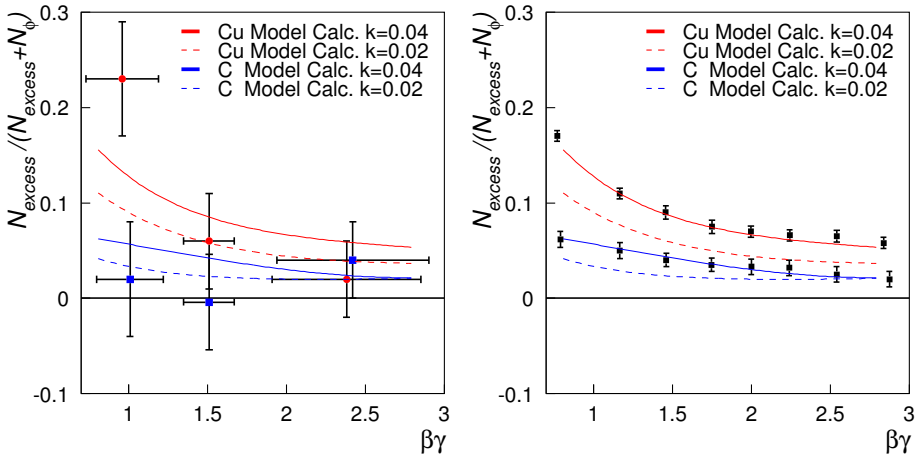

Figure 6: Left panel shows the $\beta\gamma$ dependence of the ratio $N_{excess}/(N_{excess}+N_\phi)$ observed in e^+e^- spectra measured by E325. Red circle is for copper and blue square is for carbon target data. Solid and dashed lines show the result of model calculation based on the theoretical prediction[13], red is for copper and blue is for carbon. Solid and dashed are show the two cases of parameter in the prediction. Right panel shows the effect of statistics expected in the proposed experiment. Statistical error bars will be shrunk as shown in the right panel by 100 times as large statistics as E325 which is shown in the left panel.

2.2 Goals and physics impacts

The main goal of the proposed experiment is to unambiguously measure the mass modification of mesons in cold (and hot, if heavy ion beams become available at J-PARC) nuclear matter, and approach how the hadron mass originates by spontaneous chiral symmetry breaking. With the high intensity proton beam at J-PARC, the statistics alone is expected to improve by two orders of magnitude compared to the predecessor experiment KEK–PS E325. It will allow us highly systematic approaches to how the meson mass behaves in matter.

The E325 has reported an interesting phenomenon that slower mesons generated in heavier nuclear targets exhibit higher fractions to have their

mass modified from the in-vacuum property. It suggests, or at least is consistent with, the picture that information of the modified meson mass is carried out to detection only in case the parent meson decays before escaping from the surrounding nuclear matter. That is, slower mesons taking longer time in nuclei are to decay more in the matter (and possibly modified stronger) than faster mesons. Further systematic studies are awaited to investigate the picture, and it is vital to study the collision geometry dependence of the meson mass spectrum both on the target mass and collision centrality axes, in addition to the meson velocity dependence.

When the proposed experiment collect the 100 times as large statistics as E325, the statistical error bars can be shrunk and the data binning in the meson-velocity ($\beta\gamma$) axis can be divided much more as shown in the right panel of Fig. 6. By such analysis, we will be able to approach more precise comparison with several theoretical predictions of the spectral change of vector mesons in nuclear matter.

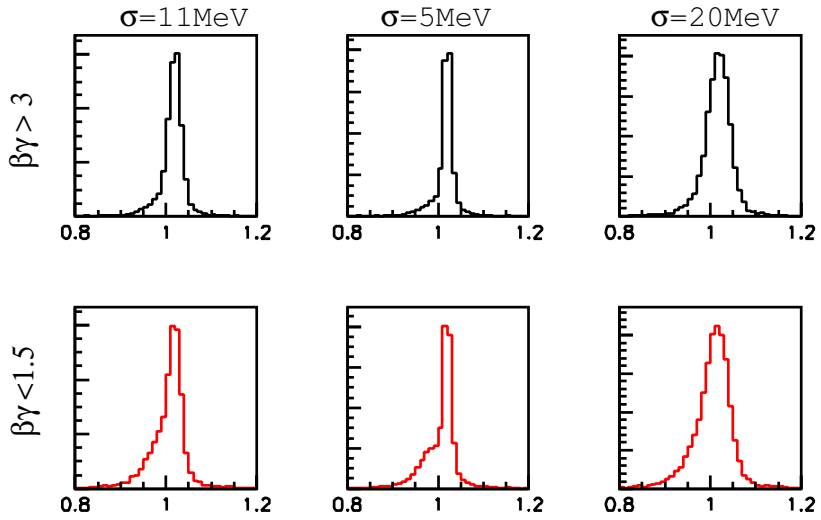

Figure 7: The expected modified invariant mass distributions of $\phi \to e^+e^-$ from Cu target with different experimental mass resolutions. Upper panels show the spectra by fast moving mesons and lowers show by slowly moving mesons.

As for the target mass dependence, a hydrocarbon target and a carbon one are planned to be bombarded by the primary proton beam, as well as heavier targets, as lead, up to A$\sim$200. Meson mass spectrum in proton-on-proton collisions will be obtained by subtracting the contribution of carbon nuclei target from the hydrocarbon data, which was given up in E325 because

of the statistical limitation. The high-statistics capability in the proposed experiment enable us to use such new targets in various size with reasonable statistical precision. The expanding the lever arm of the target mass from A=1 to A$\sim$200, in contrast to from A=12 to A$\sim$64 as in KEK–PS E325.

On the other hand, the collision geometry in p+A reaction can be measured via the charged particle multiplicity in the mid- to backward-rapidity region in the center-of-mass system, and/or via the number of so-called "grey" (slow) protons [20]. The meson velocity, the target mass, and the collision centrality dependences will play as "three arrows" and assure the systematics which is required to unambiguously understand the underlying mechanism of how the hadron mass is modified in the nuclear matter, and ultimately how it originates.

Another key to reduce systematic uncertainties is a good invariant mass resolution for the electron pairs. It enables to distinguish the possible slight tail of modified meson mass spectrum from the background. The effect of experimental invariant mass resolution on how the modified ϕ meson mass distribution looks is shown in Fig. 7. The result shows that at least approximately 10 MeV in r.m.s. at the ϕ mass, the same level as in KEK–PS E325, needs to be achieved in the proposed experiment.

3 Experimental Apparatus

3.1 Beam line

Construction of a high-momentum beam line is needed. Primary proton of 50 GeV is delivered to the beam line and beam intensity of 10^{10} per spill is needed for the proposed experiment. The beam line is originated from the SM1 separation point and the beam loss of 15 kW is allowed from radiation protection point of view.

Figure 8 shows a schematic view of the beam line. The high-momentum beam line will be constructed as the C line which originates from SM1, while the A line is the major primary beam line which has the T0 target point (for test beam lines) and the T1 target point.

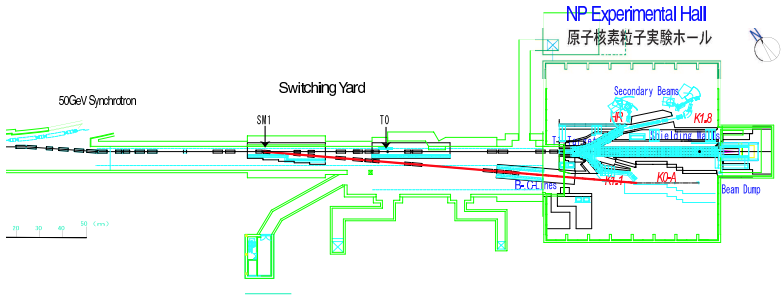

Figure 8: High-Momentum Beam Line (red line)

The beam spot size of less than 10 mm is acceptable and around 1 mm is desirable from a view point of the target(s) configuration. Less than 1 mm is not necessary taking account of heat deposit on thin targets.

The spill structure and the long time stability of intensity are also the issue. Since the experiment is performed with the high rate limit of the detector operation, stability of the beam and flat structure of the spill are very important.

The spectrometer is placed at the final focus point of the beam line as shown in Fig. 9. This spectrometer covers mainly the target region to detect the slowly moving mesons, thus the forward region is opened. Therefore the proposed spectrometer can share the beam line with other spectrometer covers the forward region. It is not favored to share the beam line with other spectrometer located just upstream our spectrometer, since the main background of the trigger is made by electrons from upstreams.

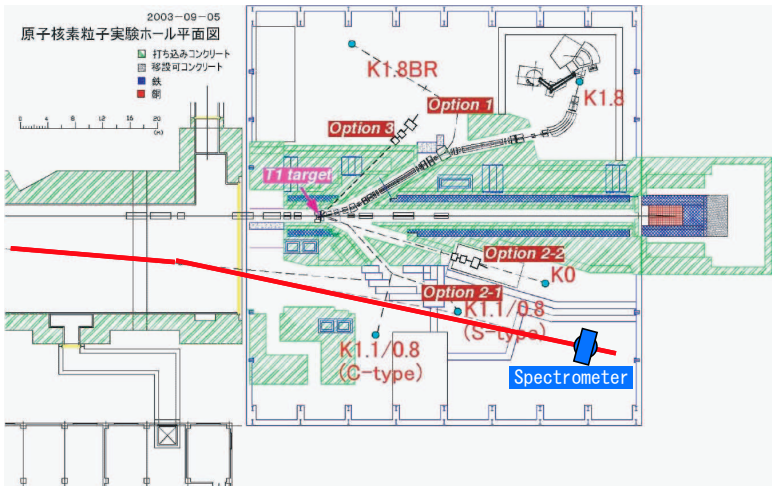

Figure 9: Counter Hall and spectrometer (blue)

3.2 Spectrometer design

The experiment is based on the same concept as E325 experiment: using thin targets ($\sim$ 0.1 % interaction) to reduce the electron background from the γ conversion in target materials, high intensity beam to cope with the thin target and small branching ratio, large acceptance spectrometer covering the backward in CM system to detect the slowly moving mesons. The proposed spectrometer keeps mass resolution and electron identification capability of E325 and has 5 times larger acceptance and works with the 10 times higher beam intensity than E325.

Name	Radius [mm]
GEM Tracker1	200
GEM Tracker2	400
GEM Tracker3	600
Čerenkov Counter	600 – 1100
Outside Tracker	1120
EM Calorimeter	1140 – 1700

Table 1: List of detectors

We propose to build a new spectrometer to cover wider geometrical acceptances as shown in Fig.10. The vertical acceptance is enlarged to $\pm 45°$. The horizontal acceptance is $0° \sim \pm 135°$ except the very forward region of

$0^\circ \sim \pm 12^\circ$ both vertically and horizontally to avoid beam halo. Schematic view of the geometrical acceptances are shown in Fig.11.

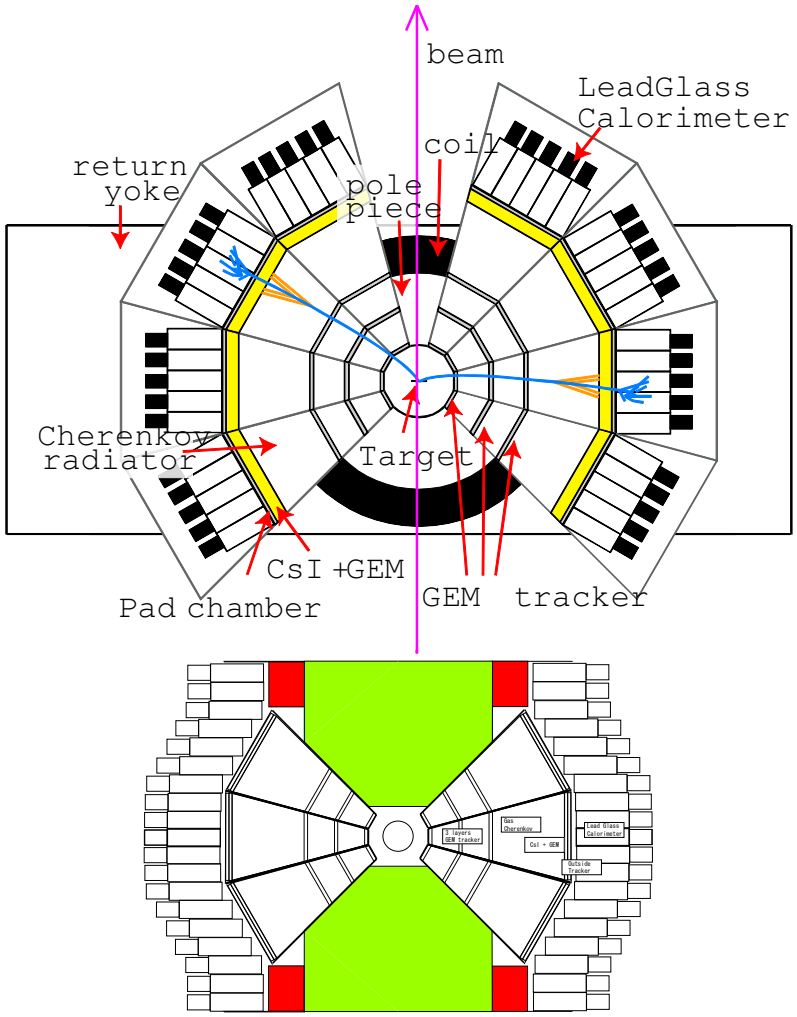

Figure 10: Schematic view of the proposed new spectrometer (plan view/beam view). Green and red area represents pole piece and coil, respectively.

The list of detectors is shown in Table 1. The spectrometer has a large magnet and detectors. We will use the same magnet used by E325. The tracking device consists of 3 layers of GEM trackers and outside tracker. Particle momentum is mainly determined by Gas Electron Multiplier(GEM) trackers. The GEM tracker is originally developed for the COMPASS experiment[21] for high rate counting and is also used at RCNP[22]. The outside tracker

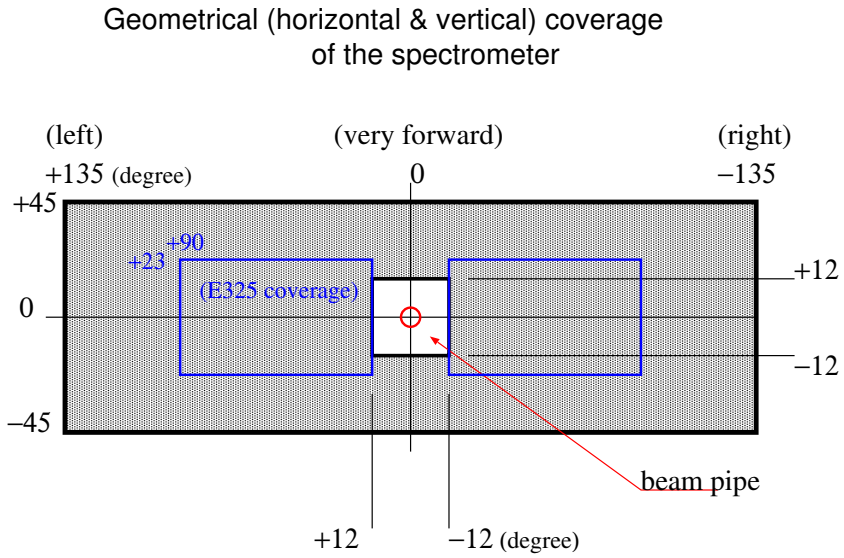

Figure 11: Schematic view of the geometrical acceptances of the spectrometer.

is pad chamber and is used for track finding and charge veto for γ measurements. Electron ID counters consist of highly segmented gas Čerenkov counter and EM calorimeter. As photon detector for the gas Čerenkov counter, CsI photo-cathode and the GEM are used. CsI photo-cathode and the GEM are being developed for the PHENIX upgrade plan[23]. Lead Glass counter is used as EM Calorimeter. The EM calorimeter segmented finer than E325 gives us a γ identification capability, thus the detection of the radiative decay of K^* and σ mesons comes into the scope.

To avoid the background from miss identification of π mesons, the rejection factor of 4.0×10^{-4} for π mesons, which is achieved at E325, is required in the momentum region of electrons from ϕ meson decays. The gas Čerenkov counter and the EM calorimeter have the rejection factor of 1.0×10^{-2} and 4.0×10^{-2}, respectively.

Multiplicity of charged particles into the tracking detectors is to be used as a measure for the collision geometry. Measurement of "grey" (slow) protons, *e.g.* below 1 GeV/c, is another option to access the collision centrality information with a higher accuracy expected. The resolution for the collision geometry is evaluated in Section 3.2.4, based on charged particle multiplicity and grey proton measurements. With the presently proposed spectrometer design and the detector configurations, the spectrometer acceptance is large enough to have a few to several grey protons, depending on the target nu-

clei and collision centrality, while the particle identification capability still requires some further consideration. In case the timing resolution of ~ 1 ns in r.m.s. of the electro-magnetic calorimeter is insufficient, a detector array based on a scintillation counter technology could be placed right in front of the calorimeter, to provide both the multiplicity and time-of-flight information for charged particles, without losing tracking and identification efficiency for electrons. The expected reaction rate of $\sim 10^7$ Hz is within the reach of conventional scintillation detectors.

3.2.1 Yield and acceptance

We estimated a yield of ϕ mesons in e^+e^- decay mode. While the estimation is done for ϕ mesons, the yield of the ρ/ω mesons is expected to be about 10 times as much as ϕ. We used the nuclear cascade code JAM[24] to estimate the production cross section and the kinematic distribution of ϕ meson in p+A reactions. It should be noted that the predictions by JAM are consistent with the results of 12 GeV p+A reaction measured by E325[7], in the kinematic distribution of ϕ meson and even in the absolute production cross section within factor 2. It was also confirmed that the incident-energy dependence of the predicted cross section by JAM is consistent with the phenomenological scaling law about production cross section of narrow vector mesons in pp reaction[25].

beam energy		12 GeV	30 GeV	50 GeV
production cross section		1.0 mb	3.0 mb	5.1 mb
detector acceptance	E325	8.8%	(6.0%)	(4.5%)
	J-PARC	45%	31%	23%
normalized yield by E325	E325	1	(2.0)	(2.6)
	J-PARC	5.1	10.0	12.7

Table 2: The ϕ meson yield in p + Cu reactions for two detector geometries.

Here, we discuss p + Cu reaction at 12 GeV, 30 GeV and 50 GeV of incident kinetic energies. The beam energy 30 GeV is planned at the Phase 1 of J-PARC, while 50 GeV is available at the Phase 2. Cross sections are scaled by the measured value at 12 GeV. The results are shown in Table 2 and Fig. 12. At 30 or 50 GeV the production cross sections are 3$\sim$5 times larger than 12 GeV, while the Lorentz boost decreases the detector acceptances for the $\phi \to e^+e^-$ detection. As a result, the yield is 10 (13) times as large as E325, for 30 (50) GeV of beam energy.

It should be noted that only the geometrical factor of the spectrometers and cross sections are considered here, in other words, the same detector/trigger/analysis efficiency, the same beam intensity ($\sim 1 \times 10^9$) and the same data acquisition periods (100 shifts) as E325 are assumed. The proposed spectrometer is designed to cope with the $\sim 1{\times}10^{10}$ proton/spill and $\sim 1{\times}10^7$ interaction/spill. Thus, the 100 times of ϕ meson yield as large as E325 can be collected in the proposed experiment.

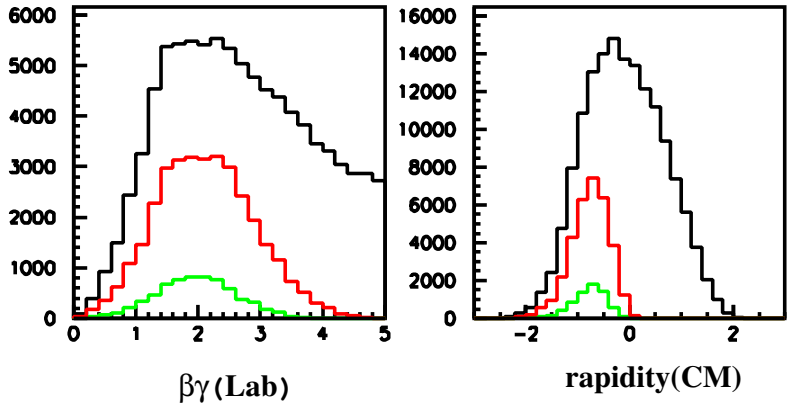

Figure 12: The ϕ meson acceptance in 50 GeV p + Cu reactions for two detector geometries. Left panels are for $\beta\gamma$ of ϕ meson in Lab system and right panels are for rapidity of ϕ meson in CM system. Black lines are for the ϕ meson distribution generated by JAM. Red lines are for the ϕ meson accepted by proposed new spectrometer geometrically. Green lines are for the ϕ meson accepted by E325 spectrometer geometrically.

3.2.2 Counting rate

The main background in E325 trigger was electrons flying from upstream whose origin may be collisions between the beam halo and materials around the beam line. For 1×10^9/spill of intensity, particle density at the point 20 mm apart from the beam line was about 350 kHz measured by the most forward cell of a E325 drift chamber with 3.5 mm of the cell width and 220 mm of height. The most forward cell located at radius of 200 mm and the horizontal angle of 6°.

The most inner layer of the new tracking device is placed at the same place as the above drift chamber. Taking account the 10 times increasing of the beam intensity and 1 sec of duration in 3 sec accelerator cycle, the maximum counting rate becomes 3.5 MHz. Note: the rate could be reduced,

since the most forward cell of the proposed chamber has the large horizontal angle of 12° and placed at the point 40 mm apart from the beam line. To cope with such high rate, the tracker has to have the 0.7 mm of the cell width and 100 mm of height. It is 10 times finer segments than the above E325 drift chamber and the counting rate per one cell reduce to 350 kHz, which corresponds to 5 kHz/mm^2. Such high rate counting can be achieved with GEM tracker and strip readout of 700 μm pitch. According to the COMPASS experiment, the detector is working up to 25 kHz/mm^2 with strips of 400 μm pitch. Taking account of the difference of the strip pitch, The proposed detector works up to 14 kHz/mm^2.

Another measurement of counting rate is done by E325 using a scintillation counter which was placed at the radius of 400 mm from 12° to 60° and has a width of 40 mm and a height of 400 mm. The courting rates of the scintillation counter at 12° and 60° are 1.8×10^6/spill and 0.4×10^6/spill, respectively.

The radius of the above scintillation counter is the same as the second layer of the proposed GEM tracker. Taking account of the 10 times increasing of the beam intensity and 1 sec of duration in 3 sec accelerator cycle, the counting rate becomes 4 MHz at the horizontal angle of 60°. Even with the drift cell whose size of 4 mm(W)× 200 mm(H) at the radius = 400 mm (for the second layer), the counting rate is 200 kHz, and for the first layer at the radius = 200 mm , 400 kHz for 4 mm(W) x 100 mm(H) of drift cell. The rates are marginal for the operation of a drift chamber, even such backward as 60°. The 4 mm of cell width is also marginal for the design of the drift chamber. Thus, we decided to use GEM trackers for all the horizontal angle region and all three layers.

3.2.3 Momentum and mass resolution

Momentum and mass resolution are evaluated using a brief simulation for the proposed spectrometer and the E325 spectrometer. The purpose of the calculation for E325 is to check the accuracy of the calculation. The simulation contains position resolution of the tracking devices and multiple scattering effects. The calculations for the proposed experiment are done with 4 position resolutions, such as 300 μm, 200 μm, 100 μm, and 50 μm. The position resolution of 300 μm is achieved with the E325 spectrometer and used in the calculation for E325. The same vertex resolution is used both for the proposed spectrometer and E325 calculation. The radiation length of the spectrometer is based on the E325 spectrometer. One layer of GEM tracker has 0.07% of radiation length. The increase of the radiation length from GEM is taken into account in the calculation. The magnetic field map as-

sumes the axial symmetry and is calculated by POISSON. The same current density is used as E325.

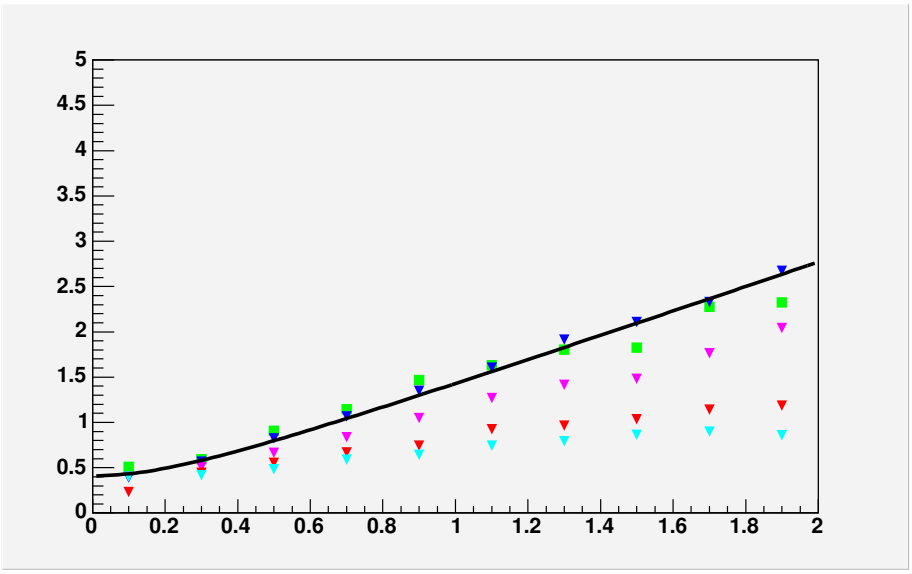

Figure 13: Momentum resolution (δp/p) as a function of momentum for E325 (green), position resolution of 300μm(blue), 200 μm(purple), 100 μm(red) and 50 μm(cyan). Black line represents achieved momentum resolution for E325.

Figure 13 shows results for momentum resolution as a function of momentum. The simulated resolution for E325 is consistent with the real value. The improvement of the chamber resolution dramatically improves the momentum resolution.

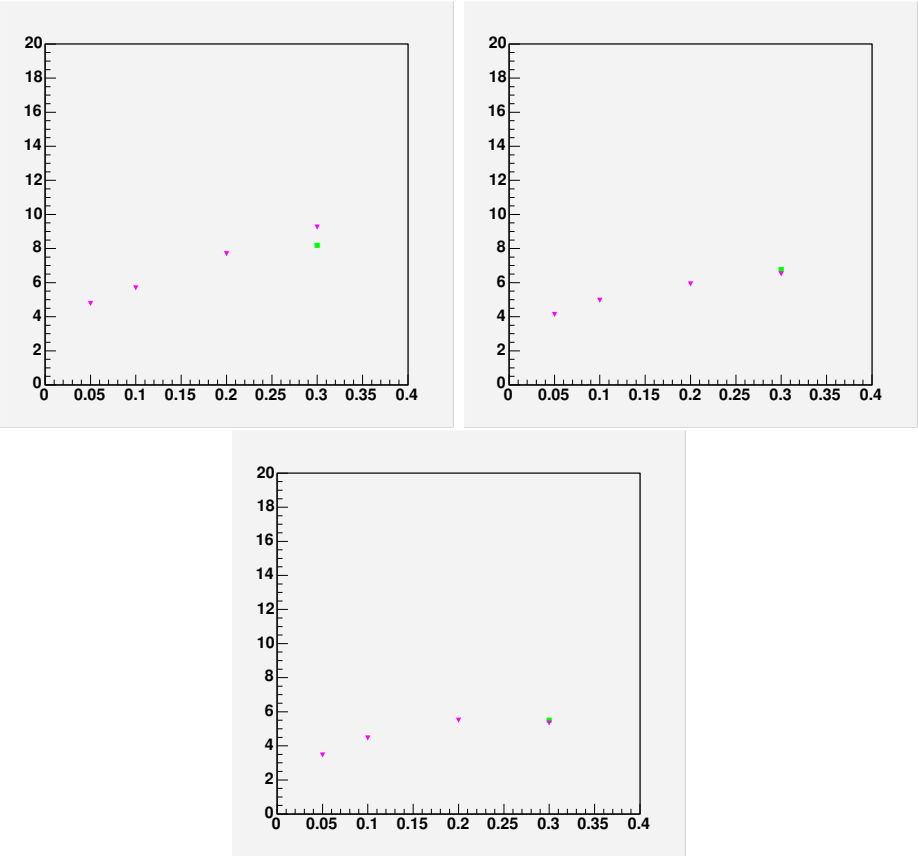

Figure 14: Mass resolution as a function of chamber resolution for all kinematics region of ϕ (Top left), $\beta\gamma < 1.25$ (Top right), and $\beta\gamma < 0.8$ (Bottom). Green points represent for E325 and purple points represents for the proposed spectrometer.

Figure 14 shows mass resolution as a function of chamber resolution. The simulated resolution for E325 (green, 8.2 MeV) is better than real value (10.7 MeV). The difference between simulation and real values is caused by the difference of magnetic field map and calibrations.

To achieve the same mass resolution as E325, the chamber resolution of 200 μm is required.

3.2.4 Collision geometry resolution

The resolution for the collision geometry, based on charged particle multiplicity and grey proton measurements, is evaluated via simulations with the JAM event generator, assuming the presently proposed spectrometer design and the detector configurations. Figure 15 shows (a) number of charged particles emitted into the aperture of the spectrometer, with an approximate low-momentum cutoff at 0.3 GeV/c by the magnetic field, (b) the same with an additional high-momentum cutoff at 1.0 GeV/c, and (c) number of protons into the aperture within the momentum range (from 0.3 to 1.0 GeV/c), in p+C and p+Pb collisions with the incident proton energy at 50 GeV, as a function of the impact parameter. Note that the selection (b) is easily achievable with the tracking system alone, while the (c) requires a moderate particle identification capability. The vertical bars indicate the dispersions, *i.e.* the distribution widths of numbers of particles. A rough classification of collision geometry, resulting in a few centrality bins, would be feasible with heavy nuclear targets such as ^{208}Pb, while it would be challenging to distinguish collision geometry with light ones as ^{12}C.

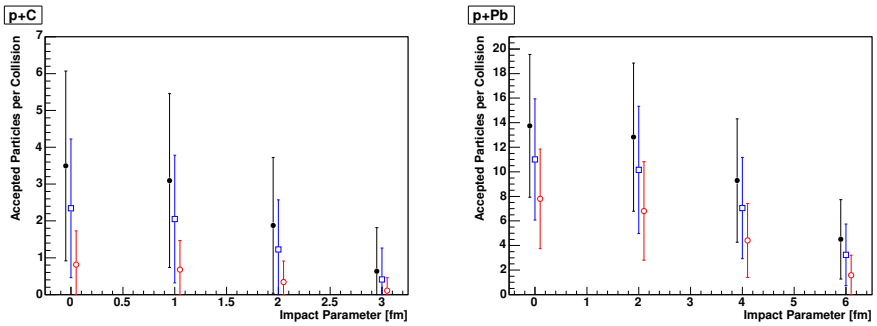

Figure 15: Evaluation of collision geometry resolution in p+C (left) and p+Pb (right) collisions at 50 GeV. Closed black circles show number of charged particles emitted into the aperture of the spectrometer with a low-momentum cutoff at 0.3 GeV/c; open blue squares are with an additional high-momentum cutoff at 1.0 GeV/c; open red circles show number of protons alone with the acceptance and momentum cuts. See text for the details.

3.3 Detector elements

3.3.1 Magnet

The magnet of the E325 spectrometer is reused for the proposed experiment. The pole piece and coil are modified to fit the larger acceptance. The schematic view of the magnet is shown in Fig. 16. The calculated magnetic

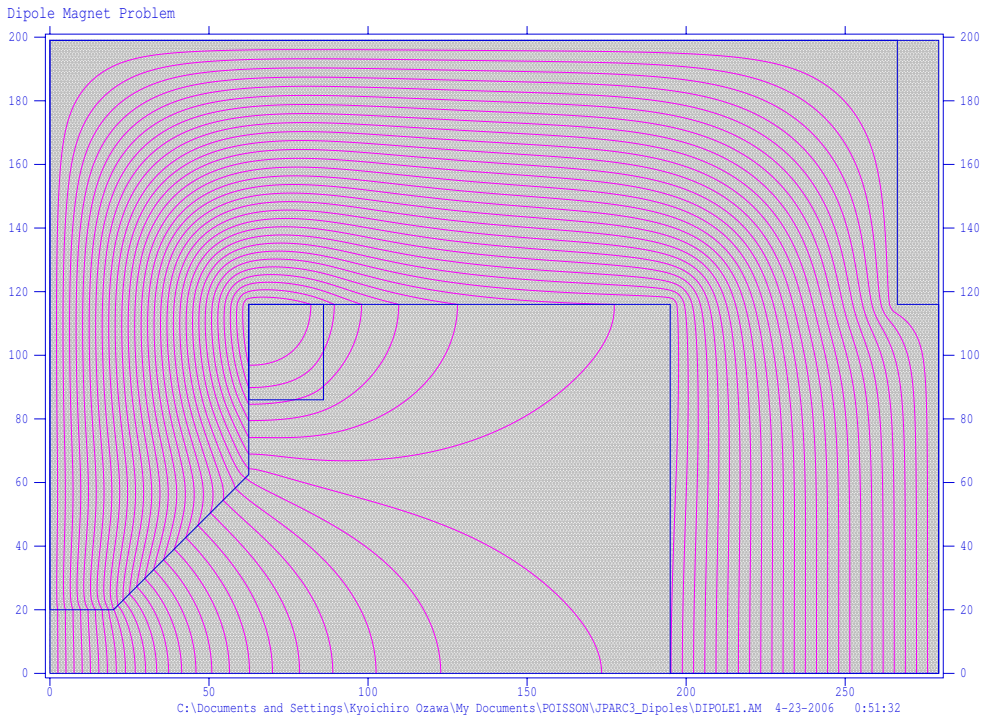

Figure 16: Schematic view of cross section of the magnet and magnetic field.

field is also shown in in Fig. 16 as red lines.

The calculation assumes the axial symmetry and is done by POISSON. The same current density is assumed as E325. Figure 17 shows field strength for the proposed and E325 spectrometer as a function of radius along y=0 plane. The change of shape of the pole piece gives us two times larger field strength than E325 at the center of the magnet.

3.3.2 Target

High statistics capability in this experiment gives us an opportunity for the systematic study of nuclear size dependence of the mass modification by using the Pb target and effective proton target by CH_2–C subtraction,

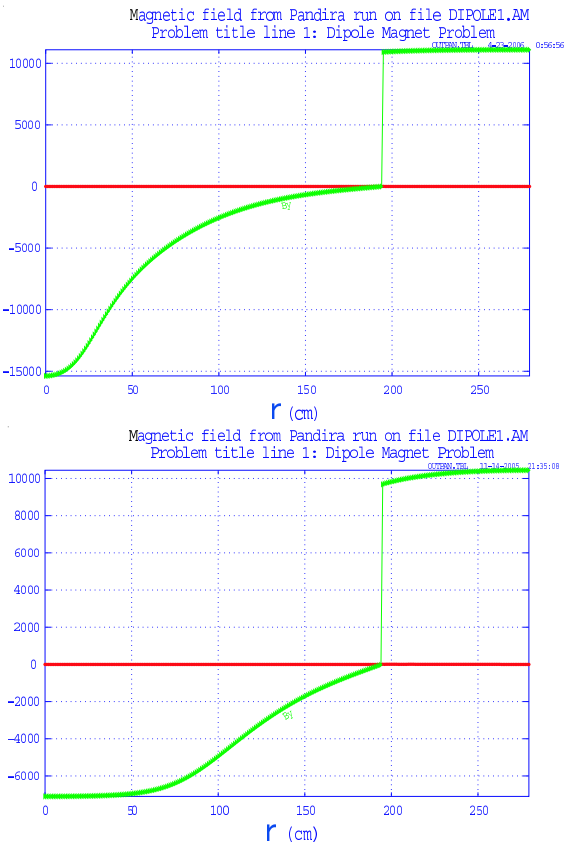

Figure 17: Field strength of y (Green) and r (Red) direction as a function of radius along y=0 plane for the proposed spectrometer (Top) and E325 (Bottom). Return yoke is located at r = 190 cm.

Typical thickness of each target foil should be around 0.5% radiation length. In such thickness of target, two main origins of the e^+e^- background have almost same number. One is the e^+e^- pair from π^0 Dalitz decays(Br=$\sim$1%) and other is the e^+e^- from the γ conversion in the target material, where γ is from the $\pi^0 \rightarrow 2\gamma$ decays(Br=$\sim$99%). It should be noted that the main background in e^+e^- spectra is the combinatorial background such that the combination of electron and positron each comes from uncorrelated two e^+e^- pairs.

Three target foils are aligned on the beam line, 20mm apart from each other, and used at the same time. Total interaction length is to be kept around 0.1$\sim$0.2%. For example, carbon foil is located at the center position and up/down stream targets are pairs of CH_2, copper or lead foils whose thicknesses are shown in the Table 3.

nuclei	interaction length(%)	radiation length(%)	thickness [μm]
C	0.05	0.1	200
CH_2	0.05	0.1	400
Cu	0.05	0.5	80
Pb	0.01	0.3	20

Table 3: target spec

Target chamber is located at the center of magnet and filled by Helium. Beam pipe from upstream is kept as vacuum and terminated by mylar window at the just upstream of the target chamber. Helium-filled pipe is located downstream the target chamber and terminated by mylar window at just outside of the spectrometer. From here to the beam dump, vacuum beam pipe is also adopted to reduce the background from the beam–gas or beam–air interaction. Target chamber should be also vacuum to reduce the background, however, large window of the target chamber to adopt the large acceptance makes it more difficult to keep the vacuum. Thin window should be used for the target chamber filled by 1 atm gas.

3.3.3 Central tracking device

GEM-based micro-pattern gas detector is used for tracking. The detectors has three layers of GEM detectors. The GEM detectors have the similar structure as developed at COMPASS [21], as shown in Fig. 18.

The GEM detectors are placed at the radius of 200mm, 400mm, and 600mm. One layer of the detector consists of three GEM foils, stacked on top of each other and separated by thin spacer grids. The electrical cloud emerging from the last GEM is collected on a readout anode comprising two perpendicular sets of strips of 700μm pitch. The total number of channel is $\sim$ 46440 for 27 segments.

The detector is divided into 9 segments horizontally and 3 segments vertically, as shown in Fig. 10 and lean to the target to make the spectrometer smaller. One segment at the most inner layer has 100mm $\times$ 100mm area.

The position resolution of 200μm can be achieved with strips of 700μm pitch. Even if there is no charge sharing between strips, $700/\sqrt{12} \sim 200$ is obtained as a spatial resolution. When the charge sharing is taken into account, the resolution is improved. In fact, the COMPASS detector achieved 71.6μm with Ar/CO2 gas and strips of 400μm pitch. Also, developed TPC-GEM at CNS has 80μm of the resolution with Ar/CH and 1.3mm pitch

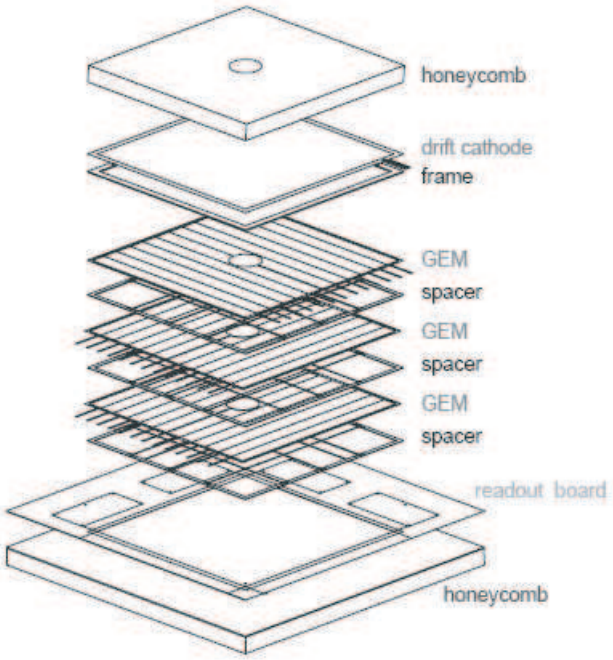

Figure 18: Exploded view of a COMPASS triple GEM detector[21].

strips[26]. Thus, we can expect better resolution than 200μm.

3.3.4 Gas Čerenkov counter

The concept of the proposed Gas Čerenkov counter (GC) is a windowless and mirror-less Čerenkov counter, operated with pure CF_4 in a proximity focus configuration. The detector consists of a 50 cm long radiator directly coupled to a triple-GEM detector which has a CsI photo-cathode evaporated on the top face of the first GEM foil and a pad readout at the bottom of the GEM stack, as shown in Fig. 19. The detector anode pad is a hexagon side of a = 15.8 mm and there are a total of 12420 pads for 27 segments. In this scheme the Čerenkov light from particle passing through the radiator is directly collected on the photo-cathode forming a circular blob image. Several kinds of R&D are already done for the PHENIX upgrade plan[23] using the same configuration and PHENIX will install the new detector in this year.

The CsI photo-cathode has large quantum efficiency in ultra violet region (100 $\sim$ 200 nm, 6 $\sim$ 11.5 eV), as shown in Fig. 20. Such large quantum

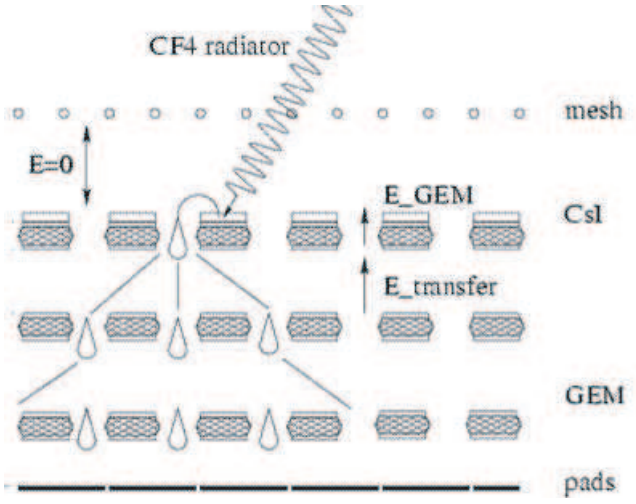

Figure 19: Schematic view of the photon detector of Čerenkov counter

efficiency gives a figure of merit N_0 =822 cm^{-1} and $\sim$ 36 photoelectrons over a 50 cm long radiator. Hadron rejection factor of 100 is achieved at the threshold of 16 electrons, as shown in Fig. 21, while preserving an electron detection efficiency larger than 90%.

3.3.5 Electro-Magnetic calorimeter

We would like to use the lead glass calorimeter (LG) modules which were used in TOPAZ experiment and has been preserved at KEK after the deconstruction of the TOPAZ spectrometer. About 650 blocks are needed to cover the acceptances of our spectrometer. They were also used in the E325 spectrometer and the rejection factor of 4.0×10^{-4} for π mesons are achieved. The rejection value is sufficient for the experiment. In addition, approximately 15% of energy resolution for 1 GeV electron was achieved. This bad resolution was due to the usage such that the particles come from the side of lead glass block in order to reduce the readout channels. In this time we expect to achieve the original energy resolution ($\sim$10% for 1 GeV electron) because of the original usage as the head-on injection to the block. By this usage, the area of trigger tile is decreased and fake electron trigger by accidental coincidence between Gas Čerenkov counter and lead glass counter could be reduced. Also, photon-measurement capability is added our spectrometer using with the charge veto described following subsection.

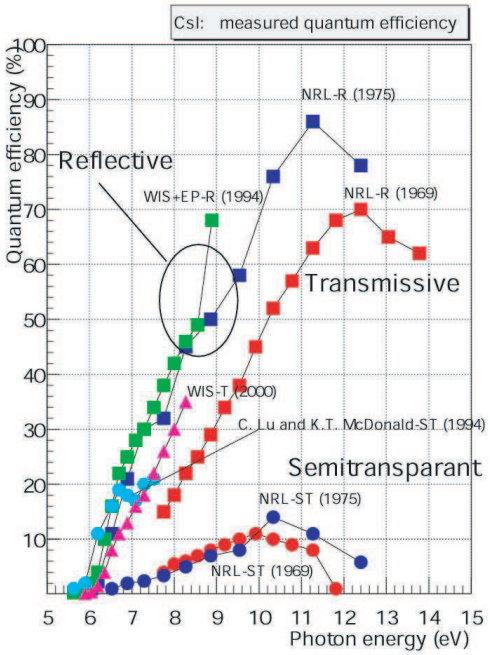

Figure 20: CsI quantum efficiency as a function of photon energy. Transmissive type is chosen at the current detector.

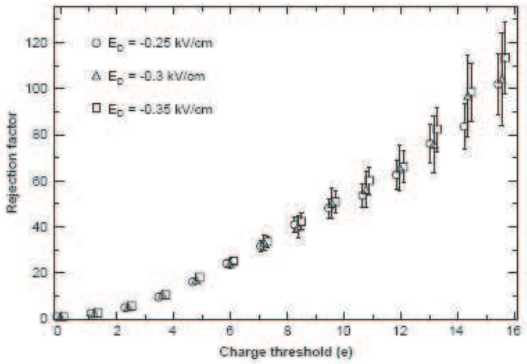

Figure 21: Hadron rejection factor using the PHENIX HBD in the test[23]

3.3.6 Outside tracker

Cathode strip chamber is used as the outside tracker to help track finding. According to E325 analysis, outside tracker greatly reduces miss trackings, while it does not contribute significantly to the momentum resolution. In addition, the detector is used for the charge veto to measure photons. The total number of channel is $\sim$ 10800 for 27 segments.

3.4 Electronics

For the readout electronics of GEM, one candidate is a hybrid preamp developed at BNL for the PHENIX experiment. The hybrid preamp, the IO1195-1, developed by the Instrumentation Division at BNL. The schematic diagram is shown in Fig. 22 It drives a differential output to a 100 ohm cable which delivers the signal to a shaper located in the Front End Module. The gain of the preamp is 6.25 mV/fC and the average output signal is 100 mV. The

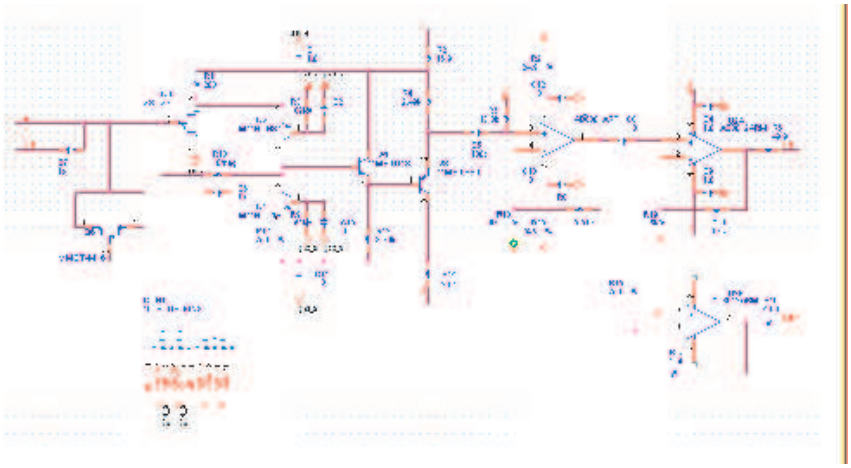

Figure 22: The IO1195-1 hybrid preamp.

noise of the preamp and current configuration is 1100 e's, which gives signal-to-noise ratio of $\sim$ 100:1 for the average input signal.

Since we have so many channels $\sim$ 70000, the dedicated front end module should be developed. The front-end module has the function of receiving the preamp signals, generating trigger primitive signal, waiting global trigger signal and digitize the preamp signals.

3.5 Trigger and background

Here we estimate whether we can conserve the first-level trigger rate as that of the E325 experiment, which was 1$\sim$2 kHz, under the 10 MHz of interaction rate which is 10 times as large as that of the E325. Our goal of the DAQ capability is several kHz with 90% of live time, which is achieved performance by the PHENIX experiment. Thus 1$\sim$2 kHz is reasonable requirement.

In the proposed experiment, main background to trigger the electron-positron pair are considered the electrons come from the upstream of the beam line and also the accidental coincidence of the electron ID counters. To trigger the electron-positron pair, first we define the electron candidate by a coincidence of a hit on Gas Čerenkov Counter(GC) and a hit on the EM calorimeter (LG) which located just after the fired pad of GC. Threshold energy of LG should be set to 0.4 GeV. Moreover we require a hit on the most outer layer of the Central tracker which roughly matches the line connecting the target and the fired LG. The rough hit position is read out from the third GEM foil of the triple-stacked structure of the GEM Tracker 3 (located most outer) which is segmented to the size of 100mm x 100mm. Lastly we require

two electron candidates which have an opening angle is larger than 60 degree at the GC pad to suppress the very low mass pair from γ conversions and π^0 Dalitz decays.

Comparing with E325 experiment, using the 10 times finer vertical information at the Central tracker and matching the line connecting the LG and the target, we can reduce the background not come from the target like as the electrons from upstream the beam line. Also 10 times finer vertical segmentation of GC and 4 times finer segmentation in LG can reduce the accidental coincidence rate of GC and LG by a factor of 40. In the proposed experiment, 10 MHz of interaction rate can cause the 10 times as high single counting rate of the electron ID counters as that of the E325 experiment. Two-fold accidental coincidence rate of the electron ID counters, which is used as the single electron candidate in the E325, could increase by 100 times. However, we have the 40 of suppression factor described above and we require even three-fold coincidence in use of the Central Tracker. Thus we can conserve the counting rate of the fake single electron and also fake pair event as same or less than the E325 experiment case, even under the 10 MHz-interaction environment.

The main background on the final e^+e^- invariant mass spectrum is the combinatorial background : the random combinations of electron and positron from the independent sources. For example, a combination of an electron from the γ-conversion in the target and a positron from a π^0 Dalitz decay. The miss-identified pions are also the origin of this background.

We estimated the combinatorial background originated from neutral and charged pions with the proposed pion rejection factor 1.0×10^{-4} and 0.5% radiation-length of target. Here, $\eta \to \gamma\gamma$ is neglected because the production cross section is smaller than that of π^0 in the order of one or two. Other hadronic sources as $\eta \to ee\gamma$, $\omega \to ee\pi^0$, etc. are also neglected because the overall effect of these hadronic sources are expected to be less than 10% of the total expected background in phi-meson mass region. The cascade code JAM is used to generate the pions in 50 GeV p + Cu interaction.

As a result, number of the random combination in our proposed detector is about 15 times as many as that of E325 with same induced-proton rate. In this acceptance and incident energy, the expected yield of ϕ meson is 10 times as large as that of E325 as described before, thus Signal-to-Noise ratio is expected to be better than the half of that of E325. It means that in the proposed experiment using the 10^{10}/spill of beam intensity, combinatorial background in the final e^+e^- spectrum comes to 150 times and number of ϕ comes to 100 times as that of the E325 case in the same length of machine time. And the number of combination accepted by the trigger is less than 200/spill for 10 M interaction/spill. In other words, not only accidental

background but also physical background cannot be negligible in the trigger rate.

3.6 Cost estimation

A brief cost estimation is shown in Table 4. In total, about five million dollars (∼600 M Yen) is required to construct the proposed spectrometer at J-PARC.

The detectors consist of 27 segments. The ±135° of horizontal coverage of the spectrometer is divided into nine and the ±45° of vertical coverage is divided into three. Thus each segment covers 30°× 30° area. The area sizes of GEM Tracker 1, 2, 3 and CsI-GEM photon detector of Gas Čerenkov counter in a segment are 10x10[cm^2], 20x20[cm^2], 30x30[cm^2] and 55x55[cm^2] respectively. Each GEM detector consists triple-stacked GEM foils. Only the first foil of GC is required to be CsI-coated as a photo-cathode.

Although the most forward segment, which is around the beam pipe, has smaller acceptance than other segments, the same number of channels are assumed for this segment in this estimation.

Detector	element	description		cost [M Yen]
			cost[Yen] (/segment)	
GEM Tracker	Frame			50
	GEM foil (10×10[cm^2] foil)	20 k $\times$(1+4+9) $\times$3	820k	23 (1134 foils)
	readout strip board (10×10[cm^2])	100 k $\times$14	1.4M	38 (378 boards)
	electronics	3 k/ch $\times$(860 $\times$2)chs	5.2M	140 (46440 chs)
Čerenkov Counter	Frame			50
	GEM foil (11×11[cm^2])	20 k $\times$25 $\times$3	1.5M	41 (2025 foils)
	CsI coat	40 k $\times$25 foils	1M	27 (675 foils)
	readout pad board		500k	14
	electronics	3 k/ch $\times$460 chs	1.4M	38 (12420 chs)
Outside Tracker	Frame			20
	readout strip board		500k	14
	electronics	3 k/ch $\times$400 chs	1.2M	33 (10800 chs)
subtotal			13.5M	
EM Calorimeter	lead glass and PMT	reuse from TRISTAN/TOPAZ		0
	Frame			20
	electronics	3 k/ch		2 (650 chs)
Magnet	Return yoke	reuse from E325		0
		transfer from KEK		30
	Pole piece	modification		20
	Coil	repair		30
Total				590

Table 4: cost estimation

4 Summary

We proposed the construction of the spectrometer at "multi-purpose high momentum beam line" at J-PARC 50-GeV PS, to measure the electron pair to investigate the chiral symmetry restoration in the finite density matter through the meson modification. At the first stage, proton induced reactions are used to investigate around the normal nuclear density. As the beam energy, both of 30 and 50 GeV are acceptable for the proposed experiment. We aim to collect around 10^5 of ϕ meson in e^+e^- decay channel and also $\rho/\omega \to e^+e^-$ more 10 times as large as ϕ. The statistics is improved by two orders of magnitude in comparison with the former experiment KEK-PS E325.

With such high statistics, we can investigate the velocity dependence of the mass spectra of vector mesons more precisely than E325, compare with various theoretical predictions and discuss the origin of the hadron mass modification in nuclear matter. We are also able to use larger and smaller size of nuclear targets as lead and proton, which cannot be used by E325 because of the statistical limitation. Then we can investigate the nuclear size effect on the mass spectra in larger and smaller target cases than that were measured in E325. By measurement of the charged particle multiplicity in the spectrometer, collision centrality can be estimated in larger target case. The dependencies of the mass spectra on the nuclear size and the collision centrality also helps to discuss the origin of the mass modification.

For definitely higher statistics and higher mass resolution than that achieved by E325, it is necessary to construct the new electron ID counters and trackers to cope with the expected high intensity beam, high interaction rate and high multiplicity interaction. For the reaction classification with the collision geometry, measurements of hadrons like grey protons are also important. In this proposal, we discussed the feasibility of the proposed spectrometer being operated under the 10 MHz of interaction-rate environment being based on the experimental experiences by the experiment KEK–PS E325.

At the next stage, other mesons like J/ψ , σ,K*, D etc. and possibly the modification of them can be measured with some upgrades of detectors and triggers. Furthermore, heavy-ion beam is used to explore the high baryon-density state in future.

References

[1] T. Hatsuda and T. Kunihiro, Phys. Rep. **247** (1994) 221
G.E. Brown and M. Rho, Phys. Rep. **269** (1996) 333

W. Cassing and E.L. Bratkovskaya, Phys. Rep. **308** (1999) 65

[2] G. Agakichiev *et al.* , Phys. Lett.**B422** (1998) 405
G. Agakichiev *et al.* , Euro. Phys. J. **C41** (2005) 475

[3] R. Arnaldi *et al.* , Phys. Rev. Lett **96** (2006) 162302

[4] K. Ozawa *et al.* , Phys. Rev. Lett **86** (2001) 5019

[5] M. Naruki *et al.* , Phys. Rev. Lett **96** (2006) 092301

[6] R. Muto *et al.* , nucl-ex/0511019

[7] T. Tabaru *et al.* , nucl-ex/0603013

[8] M.A. Kagarlis *et al.* , Phys. Rev. **D60** (1999) 025203
G.M. Huber *et al.* , Phys. Rev. **C68** (2003) 065202

[9] F. Bonutti *et al.* , Nucl. Phys. **A677** (2000) 213

[10] A. Starostin *et al.* , Phys. Rev. Lett. **85** (2000) 5539

[11] T. Ishikawa, Phys. Lett. **B608** (2005) 215

[12] D. Trnka *et al.* , Phys. Rev. Lett. **94** (2005) 192303

[13] T. Hatsuda and S.H. Lee, Phys. Rev. **C46** (1992) R34

[14] A. Hayashigaki, Prog. Theor. Phys **101** (1999) 923
A. Hayashigaki, Phys. Lett. **B487** (2000) 96

[15] F. Klingl, N. Kaiser and W. Weise*et al.* , Nucl. Phys. **A624** (1997) 527

[16] F. Klingl, T. Waas and W. Weise, Phys. Lett. **B431** (1998) 254

[17] S. Muroya, A. Nakamura and C. Nonaka, Phys. Lett. **B551** (2003) 305

[18] M. Sekimoto *et al.* , Nucl. Instrum. Meth. **A516**(2004) 390

[19] GSI/FAIR CBM experiment
`http://www.gsi.de/fair/experiments/CBM/index_e.html`

[20] I. Chemakin *et al.* , Phys. Rev. **C60** (1999) 024902

[21] B. Ketzer, Q. Weitzel, S. Paul, F. Sauli and L. Ropelewski, Nucl. Instrum. Meth. A **535**, 314 (2004).

[22] K. Fujita *et al.* , Present status of GEM detector development at RCNP, http://www.rcnp.osaka-u.ac.jp/ sakemi/mpgdWS/slide/mpgdWS_kfujita.pdf

[23] Z. Fraenkel *et al.*, Nucl. Instrum. Meth. A **546**, 466 (2005) [arXiv:physics/0502008].

[24] Y. Nara *et al.* , Phys. Rev. **C61** (1999) 024901

[25] D. Drijard *et al.* , Z. Phys. **C9** (1981) 293

[26] S.X. Oda *et al.* , IEEE Nuclear Science Symposium Conference Record (2005) 940